

Changes in prostate orientation due to removal of a Foley catheter

Dale W. Litzenberg^{a)}

Radiation Oncology, University of Michigan, Ann Arbor, MI 48109-5010, USA

Daniel G. Muenz

Department of Biostatistics, University of Michigan, Ann Arbor, MI 48109, USA

Paul G. Archer, and William C. Jackson

Radiation Oncology, University of Michigan, Ann Arbor, MI 48109-5010, USA

Daniel A. Hamstra

Radiation Oncology, Beaumont Health System, Royal Oak, MI 48073, USA

Jason W. Hearn

Radiation Oncology, University of Michigan, Ann Arbor, MI 48109-5010, USA

Matthew J. Schipper

Departments of Radiation Oncology and Biostatistics, University of Michigan, Ann Arbor, MI 48109, USA

Daniel E. Spratt

Radiation Oncology, University of Michigan, Ann Arbor, MI 48109-5010, USA

(Received 4 October 2017; revised 31 January 2018; accepted for publication 31 January 2018; published 25 March 2018)

Purpose: Investigate the impact on prostate orientation caused by use and removal of a Foley catheter, and the dosimetric impact on men prospectively treated with prostate stereotactic body radiotherapy (SBRT).

Methods: Twenty-two men underwent a CT simulation with a Foley in place (FCT), followed immediately by a second treatment planning simulation without the Foley (TPCT). The change in prostate orientation was determined by rigid registration of three implanted transponders between FCT and TPCT and compared to measured orientation changes during treatment. The impact on treatment planning and delivery was investigated by analyzing the measured rotations during treatment relative to both CT scans, and introducing rotations of $\pm 15^\circ$ in the treatment plan to determine the maximum impact of allowed rotations.

Results: Removing the Foley caused a statistically significant prostate rotation ($P < 0.0028$) compared to normal biological motion in 60% of patients. The largest change in rotation due to removing a Foley occurs about the left–right axis (tilt) which has a standard deviation two to five times larger than changes in rotation about the Sup–Inf (roll) and Ant–Post (yaw) axes. The change in tilt due to removing a Foley for prone and supine patients was $-1.1^\circ \pm 6.0^\circ$ and $0.3^\circ \pm 7.4^\circ$, showing no strong directional bias. The average tilt during treatment was $-1.6^\circ \pm 7.1^\circ$ compared to the TPCT and would have been $-2.0^\circ \pm 7.1^\circ$ had the FCT been used as the reference. The TPCT was a better or equivalent representation of prostate tilt in 82% of patients, vs 50% had the FCT been used for treatment planning. However, 92.7% of fractions would still have been within the $\pm 15^\circ$ rotation limit if only the FCT were used for treatment planning. When rotated $\pm 15^\circ$, urethra $V_{105\%} = 38.85\text{Gy} < 20\%$ was exceeded in 27% of the instances, and prostate (CTV) coverage was maintained above $D_{95\%} > 37\text{ Gy}$ in all but one instance.

Conclusions: Removing a Foley catheter can cause large prostate rotations. There does not appear to be a clear dosimetric benefit to obtaining the CT scan with a Foley catheter to define the urethra given the changes in urethral position from removing the Foley catheter. If urethral sparing is desired without the use of a Foley, utilization of an MRI to define the urethra may be necessary, or a pseudo-urethral planning organ at risk volume (PRV) may be used to limit dosimetric hot spots.

© 2018 American Association of Physicists in Medicine [https://doi.org/10.1002/mp.12830]

Key words: motion management, prostate, treatment planning, urethra

1. INTRODUCTION

There has been an increased utilization of hypofractionated radiotherapy for prostate cancer, and there is growing evidence for the safety and efficacy of more extreme hypofractionation

schedules, such as stereotactic body radiotherapy (SBRT).^{1–5}

With these ultra-hypofractionated schedules, there has been concern regarding the potential for increased toxicity, and extra measures are being investigated to minimize these potential side effects.^{1,6,7}

Prostate SBRT has been referred to by some as virtual high dose-rate (HDR) brachytherapy, due to the analogous high dose per fraction.⁸ Brachytherapy has been associated with the potential for increased genitourinary toxicity and risk for urethral structures compared to fractionated external beam radiotherapy, and similar concerns exist with prostate SBRT. To mitigate this risk, many investigators have utilized a Foley catheter during CT simulation to aid in delineating the urethra,^{9–11} given that the prostatic urethra is not readily visible during standard CT imaging. However, given the known risks of repeat Foley placement and the discomfort to the patient, many centers perform two simulation scans, one with the Foley catheter (FCT) and one without the Foley catheter as their treatment planning CT scan (TPCT). This allows for the TPCT to emulate the daily treatments without the Foley catheter, but still obtain the anatomic information on the location of the urethra.

While the prostate translations from a retrograde urethrograms have been previously studied and found to be clinically insignificant,¹² the motion and dosimetric impact of placement and removal of the Foley have not been reported. Previous studies have investigated the anatomic deformations of the prostate due to differential rectal and bladder filling over the course of therapy and found the variation compared to the treatment planning CT to be small (standard deviation <0.1 cm) compared to inter- and intrafraction translational motion.^{13–15} Other studies have measured inter- and intrafraction prostate rotations^{16–18} and the dosimetric impact of rotations.¹⁹ Many strategies have been investigated to manage prostate rotations through appropriate PTV margins,^{20–22} motion management devices,²³ rotation compensations with the table, collimator or gantry,^{24,25} and adaptive replanning.^{21,26,27}

Given the risks of catheter placement, including urinary tract infections and discomfort, we utilized data from a multi-institutional prostate SBRT study conducted from 2011 to 2013 to better determine the impact and benefit of the Foley catheter placement. The goal of the project was to investigate whether two CT simulation scans were necessary and if treatment planning could be performed on the FCT alone, or on the TPCT without a Foley at all. Reducing the number of CT scans has benefits for more efficient use of departmental resources, as it would save time and reduce imaging dose to the patient. Likewise, if a Foley were not needed, it would additionally save time and patient discomfort.

2. MATERIALS AND METHODS

2.A. Protocol eligibility

Of the 68 patients enrolled in the multicenter trial, 22 patients were consented to the IRB-approved prostate SBRT study at our institution that had both the FCT and the TPCT available (NCT01288534). The clinical results of this trial were previously reported.²⁸ All patients were 18 yr of age or older with a histologically confirmed diagnosis of adenocarcinoma of the prostate within 180 days of enrollment. Patients with PSA values of ≤ 15 ng/ml for Gleason scores of ≤ 6 , and ≤ 10 ng/ml for Gleason score of 7 were eligible

with tumor staging of T2b or less, and no plan for androgen deprivation therapy. Exclusion criteria included contraindications for electromagnetic tracking, implanted cardiac devices, metastatic disease to the lymph nodes, previous radiation, surgery, chemotherapy, or androgen deprivation therapy for prostate cancer, any significant urinary obstructive symptoms, and prostate volume of >100 cm³.

2.B. Simulation and treatment planning

Transponders were implanted a minimum of 6 days before simulation.²⁹ Patients took milk of magnesia the night before and on the morning of simulation and each treatment fraction. Additionally, a fleet's enema was self-administered 2–3 h before simulation and each treatment. Two CT scans were obtained in either the supine or prone position with a 0.1-cm image thickness. The first CT scan was obtained with a Foley catheter in place (FCT). The Foley was then removed with the patient on the CT couch and a second treatment planning CT (TPCT) scan was obtained, typically within 1–2 min after the first scan. Eleven patients were CT scanned supine with knee support, while another 11 were scanned prone on a belly board. The intraprostatic urethra was contoured on the FCT from 0.5 cm into the Foley balloon and down 0.5 cm distal to the apex of the prostate. Deformations of the prostate due to changes in rectal and bladder filling are small compared to prostate motion.^{13,15} It is assumed that the deformation of the prostate and urethra are also small due to the insertion and removal of a Foley catheter, which is a much smaller geometric perturbation than rectal and bladder changes. Consequently, the FCT and urethra were rigidly registered to the TPCT using fiducial markers (radiofrequency transponders) within the prostate. The rigid registration transformation was found with a standard least squares minimization routine employing a singular value decomposition (SVD) algorithm available in the UPlan treatment planning system. The CTV is defined as the prostate as contoured on the TPCT.

The prescription dose was 7.4 Gy/fraction \times 5 fractions to a total dose of 37.0 Gy. The PTV was defined as the prostate plus a uniform 0.3-cm margin. The PTV planning criteria were $D_{95\%} \geq 37$ Gy, $V_{115\%} < 15\%$ or 10 cc (whichever is smaller), and $D_{\max} < 120\%$. Hot spots within the prostatic urethra were limited to $D_{\max} \leq 40.7$ Gy (110%) and $V_{105\%}$ (38.85 Gy) $\leq 20\%$. Rectum constraints were $D_{\max} \leq 105\%$, $V_{100\%} < 2$ cc, $D_{90\%} \leq 10\%$, $D_{81\%} \leq 20\%$, and $D_{50\%} \leq 50\%$. Bladder constraints included $D_{\max} \leq 110\%$ and $V_{65\%} < 25\%$ or 50 cc (whichever is smaller).

2.C. Calculation of rotation from foley removal

The rigid-body registration transformation from the FCT to the TPCT was decomposed into translation and rotation components and the rotations about the left–right axis (tilt), superior–inferior axis (roll), and the anterior–posterior axis (yaw) were determined from the rotation transformation matrix,

$$R = R_{AP}(\varphi) \cdot R_{SI}(\phi) \cdot R_{LR}(\theta), \quad (1)$$

where $R_{LR}(\theta)$ denotes a tilt rotation about the left–right, X, axis by an angle θ , $R_{SI}(\phi)$ denotes a roll rotation about the superior–inferior, Y, axis, by an angle ϕ , and $R_{AP}(\varphi)$ denotes a yaw rotation about the anterior–posterior, Z, axis, by an angle φ .

To determine if these angles were larger than would be expected due to normal biological motion over the course of 1–2 min, real-time tracking data were used from the Calypso System to obtain the distribution of normal biological rotations over 1- and 2-min intervals for each patient. The change in rotation of the prostate due to removing the Foley was then compared to the patient’s distribution of normal biological rotation to determine statistical significance. Through a research agreement with Varian Medical Systems (Palo Alto, CA, USA), tracking data, including the position of all three beacons vs time (updated at 10 Hz), could be exported from the tracking system. These tracking data were obtained for each of the five treatment fractions for each patient and was used to calculate the real-time rotation angles (10 Hz) of the prostate, relative to the TPCT, during each treatment. This was accomplished with a least squares minimization routine using SVD to obtain the transformation between the measured beacon positions and the planned positions from the TPCT. The transformation was then decomposed as shown in Eq. (1) to obtain the measured rotations about each axis every 0.1 s for each of the five fractions.

The distribution of changes in rotation expected due to normal biological motion over 1 and 2 min intervals, $\Delta\theta(t)_T$, for each fraction were calculated as shown in Eq. (2).

$$\Delta\theta(t)_T = \theta(t) - \theta(t - T) \text{ where } t > T = 1, 2 \text{ minutes} \quad (2)$$

These two time intervals ($T = 1$ and 2 min) for orientation changes due to normal biological motion were evaluated to test the sensitivity of the results on time scales comparable to the variation in time between the FCT and the TPCT. While the rotations are measured in the TPCT frame, the change in rotation calculated in Eq. (2), is the change during a single fraction relative to the rotation at the beginning of that fraction. Consequently, it represents only biological motion over a treatment fraction. Any systematic changes from the orientation in the TPCT scan are subtracted out. The change in rotation of the prostate due to removing the Foley was then compared to the histogram of changes in rotation due to normal biological motion to determine the probability that the rotation due to removing the Foley was just due to normal biological motion. Because the statistical validity of adding histograms for all five fractions, which may have different systematic offsets and trends during each fraction, is questionable, the comparison was made with just the first fraction of data and all five fractions of data for each patient to test the sensitivity to this possible issue.

2.D. Determining preferred simulation CT (TPCT or FCT)

In practice, the orientation of the prostate is difficult to control, and statistically, it is possible that it might be equally or adequately represented by the FCT, justifying a single CT

TABLE I. Change in tilt, roll, and yaw angles due to removing a Foley catheter, found from rigidly registering FCT to TPCT.

Pat ID	φ (Roll) $^\circ$	ϕ (Yaw) $^\circ$	θ (Tilt) $^\circ$
p1	−1.0	1.5	−7.2
p2	0.5	5.8	12.2
p3	−3.3	8.4	−3.7
p4	−1.9	0.8	−5.9
p5	−2.9	0.5	5.0
p6	−0.3	0.2	−1.5
p7	1.9	−0.7	4.7
p8	−1.5	−0.2	−2.1
p9	−1.0	−1.1	−5.2
p10	1.6	2.9	−6.6
p11	−3.5	1.0	−2.2
Ave	−1.0	1.7	−1.1
σ	1.8	2.9	6.0
s1	−0.4	0.0	−0.1
s2	−2.1	−0.1	−0.3
s3	0.8	0.8	6.1
s4	1.2	0.0	0.1
s5	3.3	−4.7	−20.1
s6	−1.0	0.0	−0.3
s7	−1.7	2.6	4.3
s8	−0.2	0.5	1.2
s9	−0.4	0.2	5.9
s10	0.4	0.3	7.1
s11	−0.5	−0.5	−0.3
Ave	−0.1	−0.1	0.3
σ	1.5	1.7	7.4

scan, albeit with a Foley in place. The tilt angle distributions during treatment were determined from the real-time measured transponder data and the FCT-to-TPCT registration angles, for each patient relative to the FCT and the TPCT. Initial and average measured tilt angles determined from the real-time tracking data are relative to the TPCT. The FCT-to-TPCT tilt value for each patient is determined by rigid registration. The FCT-to-TPCT tilt is added to these values to obtain the average tilt of all fractions and the initial tilt of each fraction relative to the FCT. (Here it is assumed that small yaw and roll angles have minimal impact on clinical results.) The average values of tilt relative to the FCT and to the TPCT may then be compared to determine which is closest to zero.

Likewise, the initial rotation relative to the FCT and the TPCT for each fraction may be compared to the tolerance. Additionally, the number of fractions within the $\pm 15^\circ$ tolerance used in the protocol may be compared for each patient to the TPCT and the FCT orientation to determine the impact on clinical workflow.

2.E. Dosimetric impact on the urethra and prostate of the maximum allowed rotations

The potential dosimetric impact of rotations is evaluated in the context of the tolerances set for the protocol, which are

easily monitored and enforced at the beginning of each treatment fraction. For this protocol a rotational limit of $\pm 15^\circ$ was used and sets the de facto limit of dosimetric variation that's acceptable due to inter- and intrafractional rotational setup errors. The functionality within the UMPlan treatment planning system for evaluating rotational variations has been previously described and reported by Amro.¹⁹ The prostate has been shown to behave as a reasonably rigid object in the sense that geometric variations due to deformation are small compared to organ motion.^{13,15} Because the urethra passes through the prostate, and moves with the prostate, it is reasonable to infer that the same is true of the urethra and that dosimetric variations due to deformation are second-order compared to dosimetric variations caused by motion and rotation. To assess the impact of the largest rotations allowed by the protocol these new DVH curves were evaluated against the protocol constraints, PTV $D_{95\%}$, and urethra $D_{\max} < 40.7$ Gy and $V_{105\%} = 38.85$ Gy $< 20\%$, and compared (rotated minus planned DVH values) to the values from the original treatment plans. The changes in CTV $D_{95\%}$ and CTV

$D_{99\%}$ were also evaluated to assess the adequacy of the PTV margin.

3. RESULTS

3.A. Impact of foley removal on prostate rotation

Table I shows the tilt, roll, and yaw angles found by Eq. (1), in registering FCT to TPCT. Note that all angles average within $0.3^\circ \pm 7.4^\circ$ of zero for supine patients and $1.1^\circ \pm 6.0^\circ$ of zero for prone patients indicating no strong preferred rotational direction change when removing the Foley. Also note, that the standard deviation of the tilt is more than double that of the roll and yaw. Consequently, this work focused on results related to the tilt angle.

The measured real-time tilt angle of the prostate relative to the TPCT and FCT over the course of each fraction is shown in Fig. 1 for each patient. Figure 2 shows the histograms of all changes in tilt over a sliding 2-min interval during all five fractions of treatment [as calculated by Eq. (2)], along with

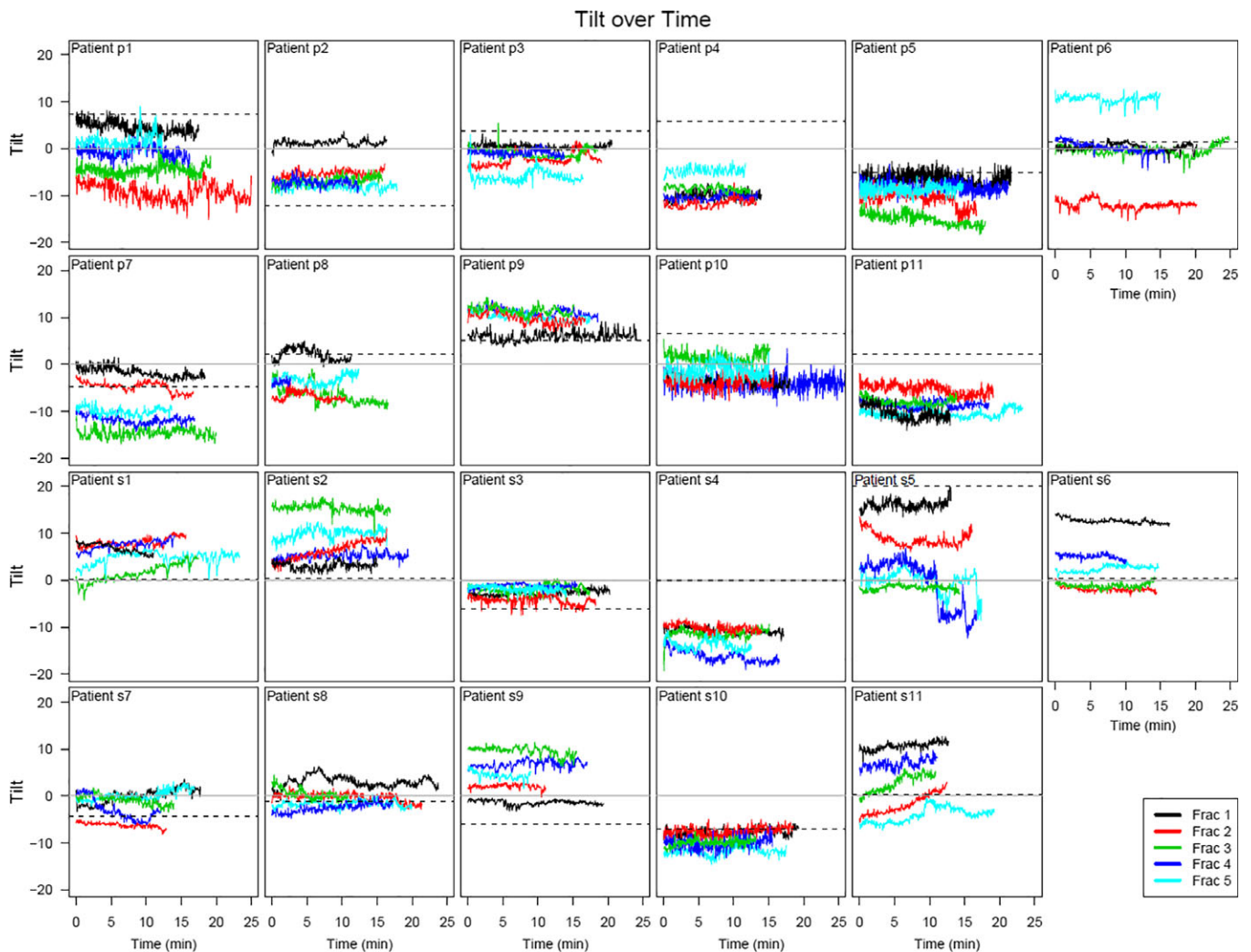


FIG. 1. Tilt angle in degrees about the left–right axis vs time relative to the TPCT (solid line at zero degrees) for each fraction of each patient. The dashed line shows the tilt of the prostate in the FCT relative to the TPCT. The top two rows show prone patients p1 through p11, while the bottom two rows show supine patients s1 through s11. [Color figure can be viewed at wileyonlinelibrary.com]

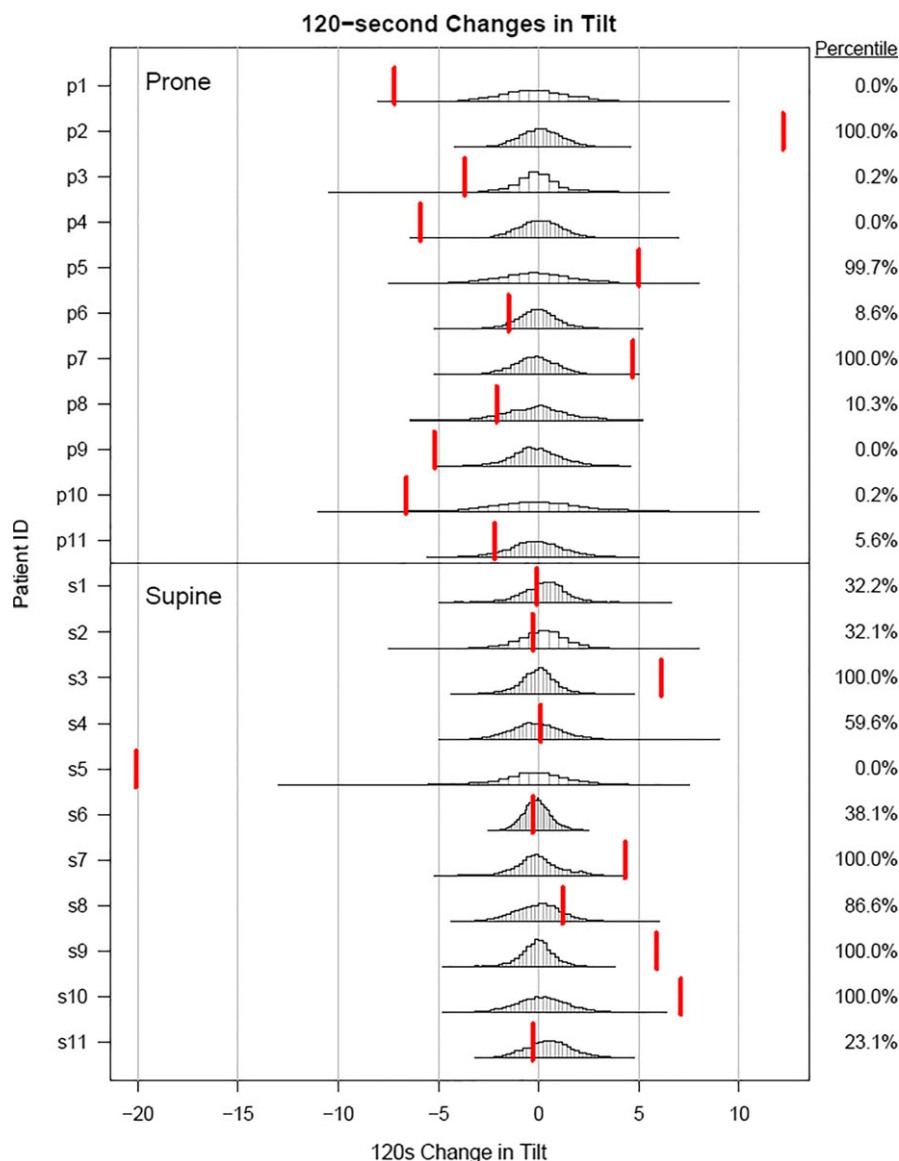


FIG. 2. Histograms of the changes in tilt over a sliding 120-s interval relative to the TPCT and the FCT (vertical mark, column 4 from Table II) for all five fractions. [Color figure can be viewed at wileyonlinelibrary.com]

the observed change in tilt from the FCT to the TPCT (dashed line). The histograms were integrated to generate cumulative density functions and the probability of the change in tilt observed between the FCT and the TPCT for each patient was determined for time intervals of 1 and 2 min, as well as for the first fraction and all five fractions, as shown in Table II.

Figure 2 illustrates that many of the tilt changes caused by removing the Foley are much larger than would be expected from normal biological motion. For the prone patients, regardless of the time interval or the number of fractions, 8 of 11 patients are outside the 95% confidence interval (i.e., <2.5%, >97.5%). If the changes in tilt due to removing the Foley were no different from normal biological motion, the probability of 8 of 11 occurrences would be 5.6×10^{-9} , assuming a binomial distribution. Likewise, 5 of 11 supine patients are outside the 95% confidence interval. If

the changes in tilt due to removing the Foley were no different from normal biological motion, the probability of 5 of 11 occurrences would be 1.1×10^{-4} . Removing the Foley caused a statistically significant prostate rotation ($P < 0.0028$) compared to normal biological motion in 60% of patients.

3.B. Rotations during treatment relative to TPCT and FCT

Figure 1 shows the tilt angle vs time for each fraction of each patient, relative to the TPCT and the FCT. These data are histogrammed in Fig. 3 which also shows the percentile of tilt angles during treatment that are less than the tilt during the FCT and TPCT (i.e., the area under the histogram in Fig. 3 to the left of the red or blue line showing the FCT or TPCT tilt angle). Eleven patients were outside the 95%

TABLE II. Percentage of naturally occurring changes in prostate tilt due to biological motion that fall below the change observed due to removing the Foley catheter, as illustrated in Fig. 3 for the right-most column in this table. Prone patient are denoted, p#, and supine patients are denoted, s#. Results are shown based on tracking data from one fraction and all five fractions, and looking at the changes in orientation over 1 and 2 min intervals. Results outside the 95% confidence interval are in bold and are independent of time interval or number of fractions.

Patient	One fraction		All (five) fractions	
	1-min interval	2-min interval	1-min interval	2-min interval
p1	0.0	0.0	0.1	0.0
p2	100.0	100	100.0	100.0
p3	0.1	0.0	0.2	0.2
p4	0.0	0.0	0.0	0.0
p5	99.4	99.1	99.8	99.7
p6	3.4	4.6	5.7	8.6
p7	100.0	100.0	100.0	100.0
p8	5.6	9.8	6.5	10.3
p9	0.0	0.0	0.0	0.0
p10	9.8	16.9	3.1	5.6
p11	0.0	0.0	0.3	0.2
s1	59.1	69.4	37.1	32.2
s2	38.2	41.1	34.0	32.1
s3	100.0	100.0	100.0	100.0
s4	57.0	58.8	57.5	59.6
s5	0.0	0.0	0.0	0.0
s6	36.2	46.8	33.6	38.1
s7	100.0	100.0	100.0	100.0
s8	82.8	76.8	89.6	86.6
s9	100.0	100.0	100.0	100.0
s10	100.0	100.0	100.0	100.0
s11	29.2	21.1	27.5	23.1

confidence interval (i.e., <2.5% or >97.5%) relative to the FCT, vs nine patients for the TPCT, and nine patients are equally or better represented by the orientation of the FCT.

Figure 4 shows the initial measured tilt relative to the TPCT and FCT for each fraction. The average tilt for all fractions and all patients relative to the TPCT are, $-3.2^\circ \pm 6.5^\circ$, $0.1^\circ \pm 7.3^\circ$, and $-1.6^\circ \pm 7.1^\circ$ for prone, supine, and all patients, and relative to the FCT they are $-4.3^\circ \pm 6.5^\circ$, $0.4^\circ \pm 7.3^\circ$, and $-2.0^\circ \pm 7.1^\circ$, respectively. These average values are all within the commonly used rotational limits of $\pm 10^\circ$, which is the default value on the tracking system, or $\pm 15^\circ$, in the case of this protocol.²⁰ Four patients had eight fractions with initial rotations out of the $\pm 15^\circ$ tolerance relative to the FCT, while only one patient had one fraction out of tolerance relative TPCT.

3.C. Dosimetric impact on the urethra and prostate of the maximum allowed rotations

The dosimetric impact of $\pm 15^\circ$ rotations relative to the TPCT on urethra and the prostate are shown in Figs. 5 and 6,

respectively. The urethra $D_{\max} \leq 110\% = 40.7$ Gy criteria was met for all patients at both $+15^\circ$ and -15° [Fig. 5(a)], increasing by 0.66%, from 39.4 ± 0.5 Gy to 39.6 ± 0.5 Gy. However, the urethra $V_{105\%} = 38.85$ Gy < 20% planning constraint increased from an average of $3.8 \pm 3.4\%$ with no rotations, to $14.4 \pm 9.4\%$ at -15° , and to $17.6 \pm 10.5\%$ at $+15^\circ$ [Fig. 5(b)]. Nine patients exceeded $V_{105\%} = 38.85$ Gy < 20% when rotated $\pm 15^\circ$. Of the 44 dose calculations at $+15^\circ$ and -15° for the 22 patients, 12 (27%) exceeded the $V_{105\%} = 38.85$ Gy < 20% planning constraint.

Ideally, the PTV expansion is large enough to maintain adequate dosimetric coverage of the CTV under anticipated distribution of translations, rotations, and deformations. At the rotational limits of the protocol, the CTV (prostate) and PTV coverage would vary as follows. The change in CTV $D_{99\%}$ relative to the prescription dose (37 Gy) is shown in Fig. 6(a). The average changed by $-2.1 \pm 4.0\%$, from 37.1 ± 0.3 Gy to 36.3 ± 1.0 Gy. CTV $D_{95\%}$ which is used to assess clinical acceptability, would be maintained with an average reduction of only -0.2% , from CTV $D_{95\%}$ of 37.6 ± 0.3 Gy to 37.5 ± 0.4 Gy as shown in Fig. 6(b). (In only one instance (-15° rotation for patient p2) did $D_{95\%}$ drop below 37 Gy to 36.6 Gy.) As seen in Fig. 6(c), the PTV $D_{95\%}$ coverage drops $-3.5 \pm 1.6\%$ from 37.2 ± 0.3 Gy to 35.9 ± 0.6 Gy.

4. DISCUSSION

It is clear that removing the Foley catheter can cause a statistically significant change in tilt of the prostate compared to the normal biologically induced changes in prostate orientation. While the average tilt during treatment compared to the TPCT ($-1.6^\circ \pm 7.1^\circ$) and FCT ($-2.0^\circ \pm 7.1^\circ$) are very similar and well within treatment tolerances, as expected the TPCT is a better or equivalent representation of prostate tilt in 18 of 22 patients. In contrast, the FCT is a better or equivalent representation in only 11 of 22 patients. However, 92.7% (102 of 110) of the fractions would still have initially been within the $\pm 15^\circ$ rotation limit if only the FCT were used for treatment planning. Even when rotated $\pm 15^\circ$, the $V_{105\%} = 38.85$ Gy < 20% constraint was only exceeded in 27% of the instances. In these instances, the value of $V_{105\%} = 38.85$ Gy was <27%, with the exception of one patient where it ranged from 44.6% to 55.5% depending on the sign of the rotation. Importantly, dosimetric coverage of the prostate was maintained above $D_{95\%} > 37$ Gy in all but one instance for rotations of $\pm 15^\circ$. With only two patients averaging $< -15^\circ$ (-15.1° and -15.6° for patients p4 and s5) over the course of treatment relative to the FCT, loss of adequate dosimetric coverage of the prostate does not appear to be an issue if treatment planning were to be performed on the FCT.

If planning were to be done on a single CT scan without a Foley, one strategy to avoid hot spots to the urethra would be to define a generic disk-like planning organ at risk volume (PRV) encompassing the medial sagittal plane of the prostate. The dimensions would be designed to encompass the possible range of motion of the urethra due to translations and

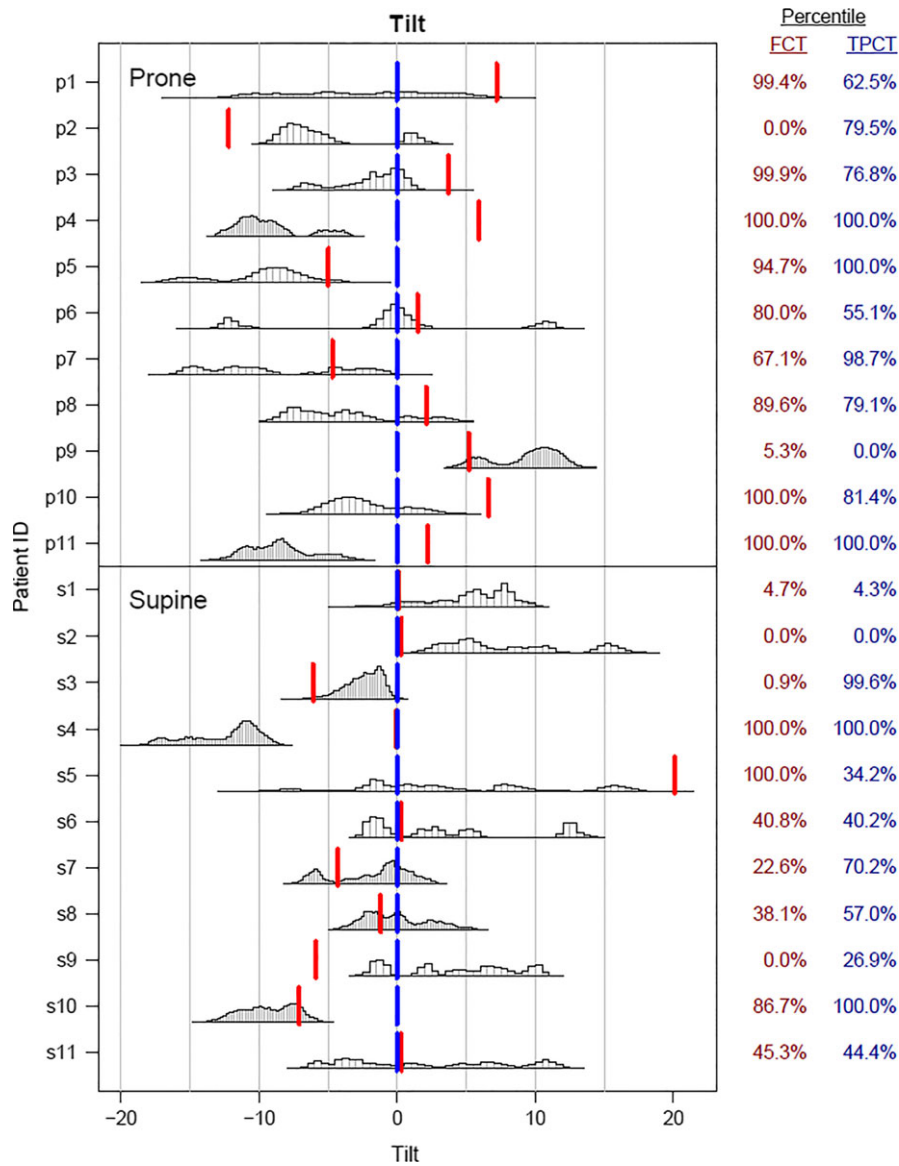


FIG. 3. Histograms of the tilt angle (degrees) of all patients relative to the TPCT (vertical mark at zero). The tilt angle of the FCT is shown by the vertical mark near or away from zero for each patient. [Color figure can be viewed at wileyonlinelibrary.com]

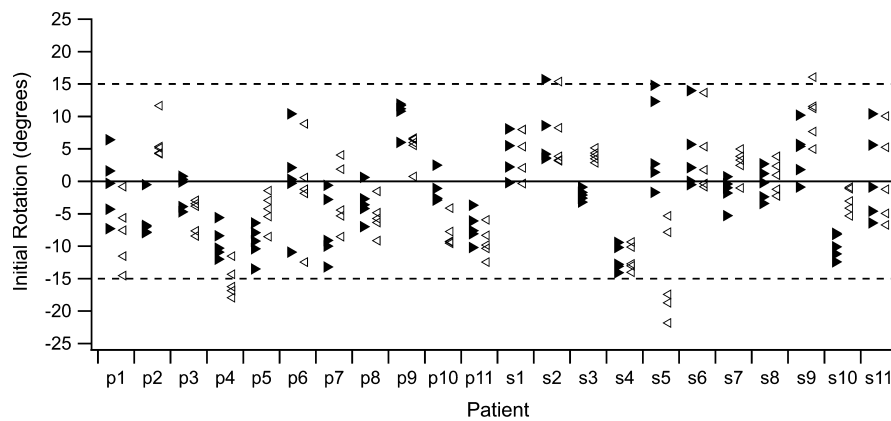


FIG. 4. This figure shows the initial tilt at the beginning of each fraction as measured relative to the TPCT (solid triangles). The values are shifted by the change in tilt measured between FCT and TPCT (outlined triangles) to illustrate the number that would have been out of tolerance relative to the FCT.

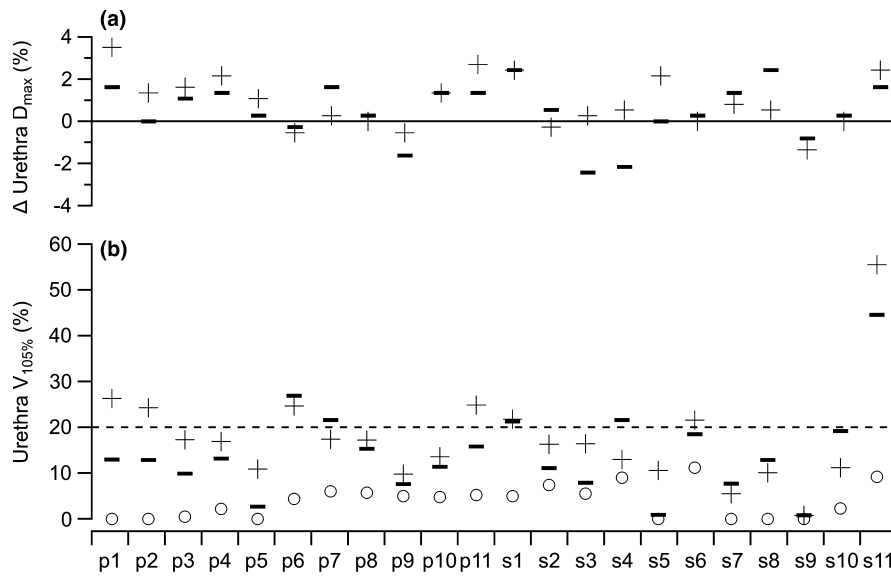


FIG. 5. Dosimetric impact on the urethra of the maximum allowed rotations. Change in the dosimetric coverage of the (a) urethra D_{max} relative to initial plan values when rotated +15° (+) and -15° (-). Figure (b) shows the planned (o) and rotated (+ and -) urethral $V_{105\%}$ values with the <20% planning constraint.

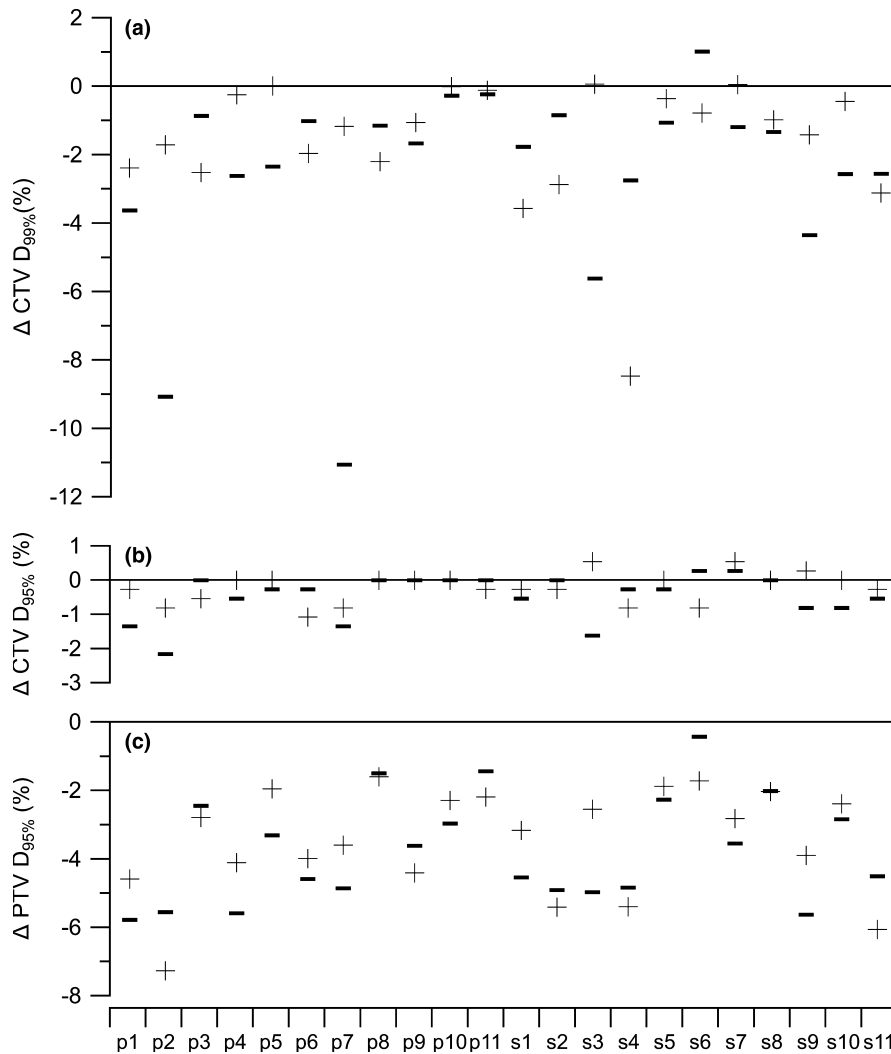


FIG. 6. Dosimetric impact on the CTV and PTV of the maximum allowed rotations. Change in the dosimetric coverage of the (a) CTV $D_{99\%}$, (b) CTV $D_{95\%}$, and (c) PTV $D_{95\%}$ relative to the prescription dose when rotated +15° (+) and -15° (-).

rotations and apply the desired dosimetric planning constraints to this structure to avoid excessive urethral dose. Additionally, investigators have demonstrated the ability to generate accurate urethral contours with the use of MRI.³⁰ It is important to note that moderate dose per fraction (7.5 Gy or less) does not result in high rates of urinary toxicity,² and some investigators have suggested the need to keep hotspots well above these dose ranges (~47 Gy).³¹ In these cases, one could safely omit the Foley catheter if hotspots are avoided in the prostate, especially in the midplane/transitional zone. However, if dose escalation to >8 Gy per fraction is used, urethral delineation likely becomes of increased importance.

While the focus of this work has been on the change in rotation caused by removing a Foley catheter, it should also be noted that changes in prostate position were also observed relative to the bones. The observed shifts (average \pm standard deviation [min – max]) were: LR = -0.05 ± 0.53 [–1.28 – 0.95] cm, AP = -0.20 ± 0.84 [–2.52 – 1.13] cm, SI = 0.03 ± 1.28 [–4.54 – 1.67] cm. Because these shifts in position can be very large relative to the surrounding anatomy, it is strongly recommended that planning should not be done on the FCT if the patient will not be treated with the Foley in place. While daily image or electromagnetic guidance would ensure acceptable dose to the target volume, the dose delivered to the neighboring organs at risk (e.g., rectum, bladder, femoral heads, penile bulb) are likely to be very different than calculated during treatment planning.

Regarding the statistical data analysis, no corrections were made for the time correlation of consecutive measurements of the tilt of the prostate, or its change over 1 or 2-min intervals. It is also unclear how valid it is to combine the changes in rotation observed between different treatment fractions. However, from Table II, it can be seen that the results are independent of the time interval (1 vs 2 min) between the two CT scans. It is also independent of whether one or five fractions of tracking data are used to determine the range of normal changes in tilt that would be expected from biological motion.

5. CONCLUSIONS

Removing a Foley catheter can cause large prostate rotations ($-1.1^\circ \pm 6.0^\circ$ for prone vs $0.3^\circ \pm 7.4^\circ$ supine patients), predominately about the LR axis, compared to normal biological changes in rotation ($P = 5.6 \times 10^{-9}$ for prone vs $P = 1.1 \times 10^{-4}$ for supine). Consequently, the TPCT is a better representation of the prostate orientation during treatment (in 82% of patients) than the FCT (50% of patients). Additionally, treatment planning optimization criteria may be employed to limit hot spots in the urethra experienced over the range of rotation allowed by protocol tolerances ($\pm 15^\circ$) while maintaining acceptable CTV coverage. This is especially true when using dose per fraction of <7.5 Gy/fraction \times 5 fractions. Doses higher than 8 Gy \times 5 may benefit from a pseudo-urethral PRV or MRI registration to limit dose to the urethra. Given the inherent risks and discomfort with

the Foley catheter placement, the need for extra dose and time from a second CT simulation scan, and the ability of treatment planning optimization to mitigate the dosimetric impact of rotations, obtaining one treatment planning scan without a Foley catheter is recommended.

CONFLICT OF INTEREST

Dr. Hamstra has received honoraria and fees from Augmenix, Myriad, Medivation, Bayer Health and Varian Medical System, and currently has a grant from Novartis. The University of Michigan has a research agreement with Varian Medical Systems that allowed access to more detailed tracking data from the Calypso System. This study was internally funded. No other authors have conflicts of interest to report.

^{a)}Author to whom correspondence should be addressed. Electronic mail: litzen@umich.edu.

REFERENCES

1. Kotecha R, Djemil T, Tendulkar RD, et al. Dose-escalated stereotactic body radiation therapy for patients with intermediate- and high-risk prostate cancer: initial dosimetry analysis and patient outcomes. *Int J Radiat Oncol Biol Phys.* 2016;95:960–964.
2. Katz AJ, Kang J. Quality of life and toxicity after SBRT for organ-confined prostate cancer, a 7-Year study. *Front Oncol.* 2014;4:301.
3. Chen LN, Suy S, Uhm S, et al. Stereotactic body radiation therapy (SBRT) for clinically localized prostate cancer: the Georgetown University experience. *Radiat Oncol.* 2013;8:58.
4. Alongi F, Fiorentino A, De Bari B. SBRT and extreme hypofractionation: a new era in prostate cancer treatments? *Rep Pract Oncol Radiother.* 2015;20:411–416.
5. Halpern JA, Sedrakyan A, Hsu WC, et al. Use, complications, and costs of stereotactic body radiotherapy for localized prostate cancer. *Cancer.* 2016;122:2496–2504.
6. Repka MC, Guleria S, Cyr RA, et al. Acute urinary morbidity following stereotactic body radiation therapy for prostate cancer with prophylactic alpha-adrenergic antagonist and urethral dose reduction. *Front Oncol.* 2016;6:122.
7. Gurka MK, Chen LN, Bhagat A, et al. Hematuria following stereotactic body radiation therapy (SBRT) for clinically localized prostate cancer. *Radiat Oncol.* 2015;10:44.
8. Spratt DE, Scala LM, Folkert M, et al. A comparative dosimetric analysis of virtual stereotactic body radiotherapy to high-dose-rate monotherapy for intermediate-risk prostate cancer. *Brachytherapy.* 2013;12:428–433.
9. Hathout L, Folkert MR, Kollmeier MA, Yamada Y, Cohen GaN, Zelefsky MJ. Dose to the bladder neck is the most important predictor for acute and late toxicity after low-dose-rate prostate brachytherapy: implications for establishing new dose constraints for treatment planning. *Int J Radiat Oncol Biol Phys.* 2014;90:312–319.
10. Fuller DB, Naitoh J, Mardirossian G. Virtual HDR CyberKnife SBRT for localized prostatic carcinoma: 5-year disease-free survival and toxicity observations. *Front Oncol.* 2014;4:321.
11. McBride SM, Wong DS, Dombrowski JJ, et al. Hypofractionated stereotactic body radiotherapy in low-risk prostate adenocarcinoma: preliminary results of a multi-institutional phase I feasibility trial. *Cancer.* 2012;118:3681–3690.
12. Liu Y-M, Ling S, Langen KM, et al. Prostate movement during simulation resulting from retrograde urethrogram compared with “natural” prostate movement. *Int J Radiat Oncol Biol Phys.* 2004;60:470–475.
13. Deurloo KE, Steenbakkers RJ, Zijp LJ, et al. Quantification of shape variation of prostate and seminal vesicles during external beam radiotherapy. *Int J Radiat Oncol Biol Phys.* 2005;61:228–238.

14. Kerkhof EM, van der Put RW, Raaymakers BW, van der Heide UA, van Vulpen M, Lagendijk JJ. Variation in target and rectum dose due to prostate deformation: an assessment by repeated MR imaging and treatment planning. *Phys Med Biol.* 2008;53:5623–5634.
15. dervan Wielen GJ, Mutanga TF, Incrocci L, et al. Deformation of prostate and seminal vesicles relative to intraprostatic fiducial markers. *Int J Radiat Oncol Biol Phys.* 2008;72:1604–1611. e1603.
16. Huang CY, Tehrani JN, Ng JA, Booth J, Keall P. Six degrees-of-freedom prostate and lung tumor motion measurements using kilovoltage intrafraction monitoring. *Int J Radiat Oncol Biol Phys.* 2015;91:368–375.
17. Lei S, Piel N, Oermann EK, et al. Six-dimensional correction of intrafractional prostate motion with CyberKnife stereotactic body radiation therapy. *Front Oncol.* 2011;1:48.
18. Aubry JF, Beaulieu L, Girouard LM, et al. Measurements of intrafraction motion and interfraction and intrafraction rotation of prostate by three-dimensional analysis of daily portal imaging with radiopaque markers. *Int J Radiat Oncol Biol Phys.* 2004;60:30–39.
19. Amro H, Hamstra DA, Mcshan DL, et al. The dosimetric impact of prostate rotations during electromagnetically guided external-beam radiation therapy. *Int J Radiat Oncol Biol Phys.* 2013;85:230–236.
20. Li JS, Jin LH, Pollack A, et al. Gains from real-time tracking of prostate motion during external beam radiation therapy. *Int J Radiat Oncol Biol Phys.* 2009;75:1613–1620.
21. Olsen JR, Noel CE, Baker K, Santanam L, Michalski JM, Parikh PJ. Practical method of adaptive radiotherapy for prostate cancer using real-time electromagnetic tracking. *Int J Radiat Oncol Biol Phys.* 2012;82:1903–1911.
22. Thomas SJ, Ashburner M, Tudor GSJ, et al. Intra-fraction motion of the prostate during treatment with helical tomotherapy. *Radiother Oncol.* 2013;109:482–486.
23. Jones BL, Gan G, Kavanagh B, Miften M. Effect of endorectal balloon positioning errors on target deformation and dosimetric quality during prostate SBRT. *Phys Med Biol.* 2013;58:7995–8006.
24. van Herten YRJ, de Kamer JBV, van Wieringen N, Pieters BR, Bel A. Dosimetric evaluation of prostate rotations and their correction by couch rotations. *Radiother Oncol.* 2008;88:156–162.
25. Rijkhorst EJ, Van Herk M, Lebesque JV, Sonke JJ. Strategy for online correction of rotational organ motion for intensity-modulated radiotherapy of prostate cancer. *Int J Radiat Oncol Biol Phys.* 2007;69:1608–1617.
26. Deutschmann H, Kametrise G, Steininger P, et al. First clinical release of an online, adaptive, aperture-based image-guided radiotherapy strategy in intensity-modulated radiotherapy to correct for inter- and intrafractional rotations of the prostate. *Int J Radiat Oncol Biol Phys.* 2012;83:1624–1632.
27. Kontaxis C, Bol GH, Lagendijk JJW, Raaymakers BW. Towards adaptive IMRT sequencing for the MR-linac. *Phys Med Biol.* 2015;60:2493–2509.
28. Jackson WC, Dess RT, Litzenberg DW, et al. A multi-institutional phase II trial of prostate stereotactic body radiation therapy (SBRT) utilizing continuous real-time evaluation of prostate motion with patient reported quality of life. *Pract Radiat Oncol.* 2018;8:40–47.
29. Litzenberg DW, Willoughby TR, Balter JM, et al. Positional stability of electromagnetic transponders used for prostate localization and continuous, real-time tracking. *Int J Radiat Oncol Biol Phys.* 2007;68:1199–1206.
30. Kataria T, Gupta D, Goyal S, et al. Simple diagrammatic method to delineate male urethra in prostate cancer radiotherapy: an MRI based approach. *Br J Radiol.* 2016;89:20160348.
31. Seymour ZA, Chang AJ, Zhang L, et al. Dose-volume analysis and the temporal nature of toxicity with stereotactic body radiation therapy for prostate cancer. *Pract Radiat Oncol.* 2015;5:e465–e472.